

An index to quantify normality of gait in young children

Maureen Tingley^a, Carla Wilson^a, E. Biden^{b,*}, W.R. Knight^a

^a *Department of Mathematics and Statistics, University of New Brunswick, Fredericton, NB, Canada E3B 5A3*

^b *Department of Mechanical Engineering, University of New Brunswick, Fredericton, NB, Canada E3B 5A3*

Received 28 June 2000; accepted 18 December 2001

Abstract

Gait patterns are often described by recording the changes in angular rotation of such joints as the hip, knee and ankle, during a complete cycle. Each joint exhibits distinctive behavior throughout the gait cycle, and abnormal gait can be described by measuring departure from a typical (mean) joint rotation curve. Standard techniques for observation of gait patterns produce large sets of data. Data reduction is achieved in this work by locating primary directions of variation from mean behavior. Variation from the mean can then be summarized with a one-dimensional statistic, thought of as a squared distance from the population mean. Percentiles of this one-dimensional index can be calculated, enabling classification of a child as normal, unusual or abnormal. A key feature of this analysis is that it is applied across multiple joint angle curves and their derivatives, thus providing a measure that takes account of the interactions between the curves as well as their individual characteristics. A data base of 348 gait cycles, collected from normal children, aged 3–7, were analyzed. Data on each child were stored in a 36-dimensional vector. Most information on patterns of variation among normal children can be stored in a smaller 11-dimensional vector, which can be used for diagnostic purposes. Performance of the one-dimensional index of gait is demonstrated on data from very young children, and on children, up to age 7, who were born prematurely. © 2002 Elsevier Science B.V. All rights reserved.

Keywords: Gait analysis; Multivariate statistics; Sagittal joint angles

1. Introduction

Gait analysis produces large amounts of data to describe movement. Typically these data include both measures such as walking speed, and gait events which are not a function of time, as well as joint angles, forces, and moments which are presented as functions of the percent of the gait cycle. In recent years principal component analysis (PCA) has become a widely used method to try to extract information from the bulk of data collected to describe gait. There has also been considerable interest in methods which can produce single indices to characterize whether a person's gait falls within the normal range.

A considerable literature exists which quantifies the mean values for various time varying measures of gait and the range of variability which may be expected in individual curves. For example, Sutherland et al. [1]

describe joint angles and their associated variability for children grouped in 10 age categories. Winter [2] provides similar data for adult and elderly gait and Lasko et al. [3] quantify the within and between person variability which may be expected in measured joint angles. These measures and reports all rely on a largely qualitative assessment of whether an individual falls within the 'normal' bounds and do not address the question of the interaction between the curves.

PCA methods provide a way to assess the deviations from the mean and interactions between curves. Deluzio et al. [4] provide a detailed description of the PCA method. They applied PCA individually to estimates of bone on bone forces, net moments and knee angles to quantify the deviation from 'normal' of individuals with osteoarthritis, using a group of asymptomatic elderly controls. Their analysis considered the entire shape of the curves, but did not provide an overall measure of the interaction between the curves. Sadeghi et al. [5] recently reported a similar analysis of flexor extensor power at the hip, but also focussed on

* Corresponding author.

E-mail address: biden@unb.ca (E. Biden).

analysis of single curves. Olney et al. [6] used a PCA technique to examine gait in people recovering from stroke, but based it on a group of 40 discrete measurements extracted from curve and single value data to characterize the gait patterns rather than on the pattern inherent in the curves themselves. An interesting note in this study was that the interpretation of the first three principal components (PCs) could be made in terms of clinical findings, but that the fourth component was ‘not interpretable’. This is not uncommon in PCA analysis, since combinations may be, as Olney et al. [6], found very difficult to interpret. Schutte et al. [7] address this issue in searching for an ‘index’ of gait by choosing their set of variables to analyse from a group of observations which have been pre-screened by clinicians to be ones which are likely to be useful in detecting changes in gait. On the other hand, their method considers only discrete variables and not time varying ones other than through features extracted, such as maximum values or ranges of motion. Related work reported by Schwartz et al. [8], uses discrete data drawn from motion analysis data related to the hip joint to establish a means to put a single ‘score’ on hip flexor function.

In this paper we describe a method which allows consideration of multiple curves simultaneously in the creation of a ‘score’ which describes how far a person’s gait deviates from ‘normal’. We consider as our example, sagittal joint angles for the hip, knee and ankle. These angles are straightforward to measure and are quite consistent across different gait analysis systems (Biden et al. [9]) thus making it feasible to use the results reported here on new data. Our goal is to describe both the typical variation from the mean seen in a normal population as well as variations from the mean which are indications of pathological gait. From the point of view of the statistics, we seek measures which spread the data out and produce clear distinctions between normal and abnormal conditions. We began using PCA but found, as Olney et al. [6] noted above, that the components were difficult to interpret. For that reason we propose an analysis which uses data which are relatively easy to interpret, and assess how well they compare to PCA. Some of the measures we suggest, angular velocity and acceleration, are not commonly used as direct measures of gait. However examples of work such as that of Granata et al. [10] suggest these may be, in themselves, clinically valuable measures. We have used an established data set (Sutherland et al. [1]) to define the variations present in normal gait. Then we have used data from children born prematurely, and who have a high likelihood of abnormal movement patterns, to demonstrate the effectiveness of the measures when applied to other children.

This paper is organized with the description of the methods and results in the body and the mathematical development included in an Appendix A at the end.

2. Methods

Gait data, specifically sagittal plane joint angles, from Sutherland et al. [1] were used to define the normal patterns for the hip, knee, and ankle in the sagittal plane. We used similar data from another study by Sutherland (National Institute of Child Health and Human Development grant R01HD015801, 1981–1984) on children who had been born prematurely, but at appropriate weight for their gestational age, for demonstration of the technique to be developed.

Work by Sutherland et al. [1,11] suggest that gait patterns are maturing by age 3 years. For this analysis, we used data from 174 gait studies performed on children in the 3–7 year old age range. Data from the sagittal plane joint rotations (hip flexion, knee flexion, and ankle flexion) were used. Work by Lasko et al. [3] suggests that, for individual joint angles, the variability from cycle to cycle for one child has roughly 1/4 the amplitude of the variability for a group of children of similar age. For this reason, the 174 left sides and 174 right sides, were combined as one set of 348 observations, indexed as $i = 1, \dots, 348$ ‘cycles’. This approach does not bias estimation of the mean but, by pooling the ‘between child’ variation with the ‘within child’ variation, variances may be underestimated. For each cycle, a set of T frames were chosen corresponding to (approximately) evenly spaced time periods throughout the cycle (T between 15 and 24). At each of the T times, hip flexion/extension, knee flexion/extension and ankle dorsi-/plantar- flexion were found.

There is no obvious way to compare, statistically, the set of angle displacements of a cycle with one number of frames (T) to another cycle with a different number. To address this, we approximate the curves using Fourier series having the same number of coefficients for every cycle (Capozzo et al. [12], Sutherland et al. [11], Olshen et al. [13]). Using Fourier series amounts to performing a least squares regression of the angle displacement values $f(t)$ (where t is scaled so that 0–1 represents 0–100% of the gait cycle). See Eq. (1) in Appendix A. Six harmonics were used in this analysis. Olshen et al. [13] determined that harmonics higher than six contain almost no information and work as early as Capozzo et al. [12], used six harmonics in their finite Fourier approximations.

Each joint has a pattern of motion, characterized by the Fourier coefficients, α_j and β_j , $j = 1, 2, \dots, 6$, and an average angular value, α_0 . The term α_0 has been omitted from subsequent analyses. That is to say, we describe the pattern of each child’s angle displacement about his/her own average displacement. As noted elsewhere (Biden et al. [14]) average displacement is more prone to error from marker position differences from person to person than is the pattern of motion. Fig. 1 illustrates the raw data (shown as points) and the estimated

right knee flexion/extension curve $f(t)$ for Child 8002, showing a very good approximation.

The statistical analyses use, as input data, the vectors $\Gamma^{(i)} = (\gamma_h, \gamma_k, \gamma_a)$ which represent the three sets of Fourier coefficients (hip, knee and ankle) describing each child. Fig. 2 shows the mean hip, knee and ankle curves, calculated over the data base of 348 cycles. The task here is to determine, for a given 36-dimensional record, $\Gamma^{(i)}$, whether the cycle is to be classified within the bounds for normal gait, or as abnormal. To reduce the volume of data, we began by using the PCA technique as used in gait analysis by others noted above. The analysis involves searching through the multi-dimensional observations looking for ‘directions’ in which the data exhibit most variability. This search uses standard techniques of linear algebra to find eigen vectors of the estimated covariance matrix, Σ_G , of the $\Gamma^{(i)}$. See Eq. (2) in Appendix A, and Seber [15]. The PCs are linear combinations of the original variables and collectively represent orthogonal directions (directions at right angles to one another) in the 36-dimensional space of the original variables. Geometrically, the first PC describes

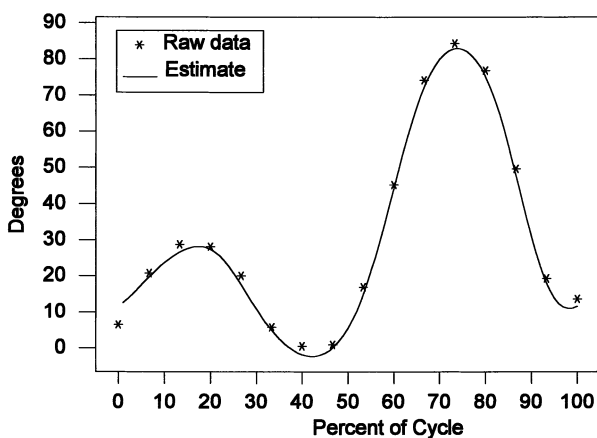


Fig. 1. Raw data and estimated knee flexion extension, right side, Child 8002.

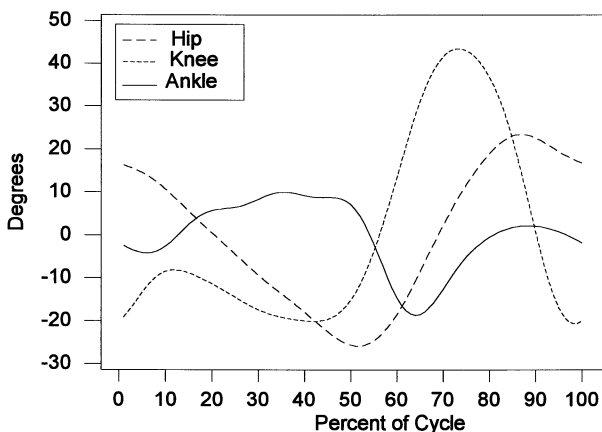


Fig. 2. Normal (mean) hip, knee and angle patterns.

a line: it is the line which minimizes the sum of squared perpendicular distances from the original 348 data points to a line in 36-space. The first PC describes the direction of greatest variation within the data set. The second PC records the direction of the next largest variation, at right angles to the first PC, and so on. The total number of PCs that can be computed in any problem is equal to the dimension of that problem (in this case, 36). Schutte et al. [7] provide an excellent graphical description of how to interpret PCs.

The PCA was performed using the SAS[®] procedure, PROC PRINCOMP. Use of the covariance matrix Σ_G assumes that the amount of variation displayed by a component of $\Gamma^{(i)}$ is correlated positively with its importance. For example, the values γ_k (knee flexion) are generally larger, with greater variation, than those of γ_a (ankle flexion). The PCA tends to choose directions which give greater emphasis to components of knee flexion than to components of ankle flexion. Note that the PCA could have used the correlation matrix (obtained by ‘standardizing’ Σ_G to have diagonal entries equal to 1). If the correlation matrix were used, then knee flexion/extension and ankle flexion would be given equal weight. If the various uncontrolled measurement errors are equal in size for all angle rotations, then the larger measurements, such as γ_k are relatively more accurate than smaller measurements. For this reason, the PCA was performed on the covariance matrix, Σ_G .

The first four PCs calculated by SAS[®] explained 72.7% of the total variation in the data and the first eight explain 85.7%, which is comparable to the results reported by Olney et al. [6] and Sadeghi et al. [5] The behaviour of the PCA provides a ‘yardstick’ against which to compare ‘interpretable functions’. The objective for the interpretable functions was to explain at least 70% of the variation in the data, and to capture variation in directions similar to those captured by the PCA.

The set of 11 interpretable functions, which explain 74.8% of the variation in the 36 dimensional data base, is listed in Table 1, and their numeric values are listed in Table 2. The decision to use 11 interpretable functions is arbitrary (as is the choice of the number of PCA’s). We have chosen enough functions to explain about 70% of the variability. The 11 interpretable functions describe mean trends in the data base. Three of these function describe mean hip motion (normal hip angle pattern (HAP), normal hip angular velocity (HAV), and normal hip angular acceleration (HAA)); and four functions each describe mean ankle and knee motion (angle pattern, angular velocity, angular acceleration, and primary frequency—the values of α_1 and β_1). The non-zero entries in the first column of Table 2 describe Fourier coefficients $\alpha_1, \dots, \alpha_6, \beta_1, \dots, \beta_6$ for mean hip angle pattern. When those coefficients are used in Eq.

Table 1
Description of the 11 interpretable functions

Function	Description	Abbreviation
I	Normal hip angle pattern	HAP
II	Normal knee angle pattern	KAP
III	Normal ankle angle pattern	AAP
IV	Normal hip angular velocity	HAV
V	Normal knee angular velocity	KAV
VI	Normal ankle angular velocity	AAV
VII	Normal hip angular acceleration	HAA
VIII	Normal knee angular acceleration	KAA
IX	Normal ankle angular acceleration	AAA
X	Primary frequency of normal knee angle pattern	PFK
XI	Primary frequency of normal ankle angle pattern	PFA

(1) in Appendix A for $f(t)$, the graph of f will be the same as that shown in Fig. 2 for the normal hip angle pattern. Angular velocity and acceleration can be interpreted intuitively as measures first of how fast the angular position is changing (angular velocity), and then as the rate of change of the change (acceleration). For example, referring to Fig. 2, normal knee flexion (coefficients listed in the second column of Table 2) increases as the leg is loaded at the beginning of the cycle, decreases in mid-stance, and shows a rapid increase starting at about the 50% point of the cycle preparatory to toe off. Fig. 3 shows the mean pattern for knee angular velocity: values are initially positive, then negative, then much more positive starting at about the 50% point of the cycle. In Fig. 3, there is a rapid decrease in velocity values between the 60 and 85% points of the cycle. From this we can infer that the graph of normal knee angular acceleration will take (relatively large) negative values in the period 60–85%

Table 2
Numeric values of interpretable functions Q

Row	HAP	KAP	AAP	HAV	KAV	AAV	HAA	KAA	AAA	PFK	PFA
1	21.44	0.00	0.00	-7.07	0.00	0.00	-21.44	0.00	0.00	0.00	0.00
2	-3.98	0.00	0.00	-6.45	0.00	0.00	15.94	0.00	0.00	0.00	0.00
3	-0.14	0.00	0.00	4.13	0.00	0.00	1.23	0.00	0.00	0.00	0.00
4	-0.46	0.00	0.00	-0.07	0.00	0.00	7.32	0.00	0.00	0.00	0.00
5	-0.07	0.00	0.00	1.89	0.00	0.00	1.78	0.00	0.00	0.00	0.00
6	-0.04	0.00	0.00	0.91	0.00	0.00	1.48	0.00	0.00	0.00	0.00
7	-7.07	0.00	0.00	-21.44	0.00	0.00	7.07	0.00	0.00	0.00	0.00
8	-3.23	0.00	0.00	7.97	0.00	0.00	12.90	0.00	0.00	0.00	0.00
9	1.38	0.00	0.00	0.41	0.00	0.00	-12.39	0.00	0.00	0.00	0.00
10	-0.02	0.00	0.00	1.83	0.00	0.00	0.29	0.00	0.00	0.00	0.00
11	0.38	0.00	0.00	0.36	0.00	0.00	-9.45	0.00	0.00	0.00	0.00
12	0.15	0.00	0.00	0.25	0.00	0.00	-5.47	0.00	0.00	0.00	0.00
13	0.00	-1.10	0.00	0.00	-25.46	0.00	0.00	1.10	0.00	-1.10	0.00
14	0.00	-15.98	0.00	0.00	11.77	0.00	0.00	63.93	0.00	0.00	0.00
15	0.00	-1.11	0.00	0.00	13.47	0.00	0.00	10.00	0.00	0.00	0.00
16	0.00	-1.71	0.00	0.00	4.51	0.00	0.00	27.35	0.00	0.00	0.00
17	0.00	-0.24	0.00	0.00	5.92	0.00	0.00	5.90	0.00	0.00	0.00
18	0.00	0.03	0.00	0.00	2.03	0.00	0.00	-1.14	0.00	0.00	0.00
19	0.00	-25.46	0.00	0.00	1.10	0.00	0.00	25.46	0.00	-25.46	0.00
20	0.00	5.89	0.00	0.00	31.96	0.00	0.00	-23.55	0.00	0.00	0.00
21	0.00	4.49	0.00	0.00	3.33	0.00	0.00	-40.40	0.00	0.00	0.00
22	0.00	1.13	0.00	0.00	6.84	0.00	0.00	-18.05	0.00	0.00	0.00
23	0.00	1.18	0.00	0.00	1.18	0.00	0.00	-29.61	0.00	0.00	0.00
24	0.00	0.34	0.00	0.00	-0.19	0.00	0.00	-12.17	0.00	0.00	0.00
25	0.00	0.00	-0.43	0.00	0.00	7.41	0.00	0.00	0.43	0.00	-0.43
26	0.00	0.00	0.56	0.00	0.00	-14.28	0.00	0.00	-2.22	0.00	0.00
27	0.00	0.00	-3.63	0.00	0.00	1.25	0.00	0.00	32.70	0.00	0.00
28	0.00	0.00	1.61	0.00	0.00	-0.53	0.00	0.00	-25.71	0.00	0.00
29	0.00	0.00	-0.43	0.00	0.00	-5.83	0.00	0.00	10.75	0.00	0.00
30	0.00	0.00	0.45	0.00	0.00	2.40	0.00	0.00	-16.15	0.00	0.00
31	0.00	0.00	7.41	0.00	0.00	0.43	0.00	0.00	-7.41	0.00	7.41
32	0.00	0.00	-7.14	0.00	0.00	-1.11	0.00	0.00	28.56	0.00	0.00
33	0.00	0.00	0.42	0.00	0.00	10.90	0.00	0.00	-3.75	0.00	0.00
34	0.00	0.00	-0.13	0.00	0.00	-6.43	0.00	0.00	2.10	0.00	0.00
35	0.00	0.00	-1.17	0.00	0.00	2.15	0.00	0.00	29.16	0.00	0.00
36	0.00	0.00	0.40	0.00	0.00	-2.69	0.00	0.00	-14.37	0.00	0.00

Values of $\alpha_1, \dots, \alpha_6$ and β_1, \dots, β_6 describing Fourier curves.

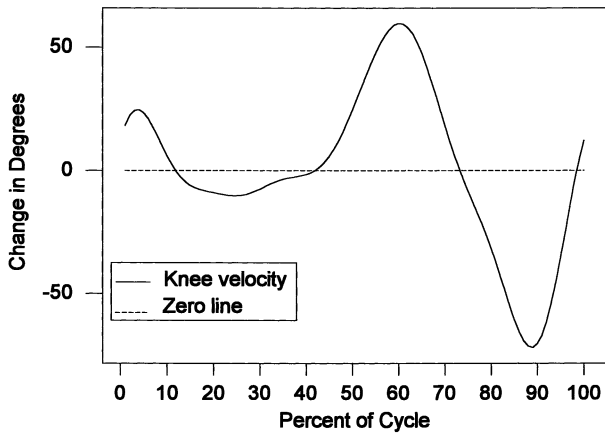


Fig. 3. Normal (mean) knee angle velocity.

of the cycle. The coefficients for HAV listed in column 4 of Table 2 describe the first derivative of mean hip flexion, and the coefficients of HAA (column 7) describe the second derivative. In each case a scaling factor of either 2π for HAV or $(2\pi)^2$ for HAA has been applied. (Directions are determined only by the relative size of non-zero entries in each column of Table 2, so that re-scaling is permitted.) It is a useful characteristic of Fourier series that the derivatives of sin and cos are proportional to cos and $-\sin$ for the same angular values. To illustrate: since the derivative (with respect to t) of $\alpha_j \cos(j2\pi t)$ is $-j2\pi\alpha_j \sin(j2\pi t)$, the third sine (row 9) term for the equation describing HAV rounds to 0.41, which is minus 3 times the third cosine term (row 3) in the hip angle equation HAP, -0.14 (Similarly, compare row 9 of HAA with row 3 of HAV, etc.).

Any one cycle has hip, knee and ankle patterns which differ from the mean curves described by the first three interpretable functions. A child's pattern of variation from the normal hip, knee and ankle pattern curves can be approximated as a linear combination of the 11 interpretable functions in a manner exactly like using PCA. That is to say, a set of curves describing an individual's departure from the mean can be approxi-

mated by adding and subtracting multiples of that mean and other mean curves. The multiples, represented by a vector $B^{(i)}$ to be added and subtracted, vary from child to child, and the size of those multiples can be used to diagnose abnormalities (Eq. (3) in the Appendix A). The remarkable property of the 11 interpretable functions is this: these patterns of average behaviour also capture directions in which individuals tend to depart from average patterns.

The interpretable functions overlap the directions of the first, second and fifth PCs (regression R^2 above 0.80 for regression of each PC on the 11 interpretable functions), but seem to be capturing different directions than the other PC's (R^2 values 0.59, 0.42, 0.41, 0.66, and 0.18, respectively for PCs 3, 4, 6, 7, 8). Nevertheless, there is evidence (presented below) that the interpretable functions perform at least as well as the (uninterpretable) PCs for diagnostic purposes.

In order to determine 'normal' and 'abnormal' gait patterns, first calculate $B^{(i)}$ for each entry in the original data set, and then calculate the covariance matrix for all 348 11-dimensional $B^{(i)}$ (see Appendix A for a description). The new (11×11) covariance matrix is denoted by Σ_B . The diagonal entries of Σ_B are variances of the 11 components of the $B^{(i)}$, and the off-diagonal entries are covariances. The inverse matrix is denoted by Σ_B^{-1} . These two matrices are printed in Tables 3 and 4. We supply these matrices to allow others to apply these results directly. In particular the inverse matrix is very sensitive to the accuracy with which numbers in the covariance matrix are represented. These matrices may be downloaded from www.math.unb.ca/~maureen/Gaitdata.

An individual's data are transformed into the one-dimensional measure $D^{(i)}$, using Eq. (4) in Appendix A. With reference to Table 3, the largest variance (diagonal entry) in Σ_B is exhibited by the primary frequency of the normal ankle angle pattern (PFA). The smallest variance is shown to be for the normal ankle angular acceleration (AAA). As Σ_B^{-1} is used in

Table 3
The matrix Σ_B

	HAP	KAP	AAP	HAV	KAV	AAV	HAA	KAA	AAA	PFK	PFA
HAP	0.0256	0.0045	0.0100	0.0004	-0.0060	0.0034	0.0050	0.0005	0.0002	0.0071	-0.0017
KAP	0.0045	0.0400	-0.0024	0.0047	0.0096	0.0062	-0.0017	0.0042	-0.0012	-0.0386	0.0024
AAP	0.0100	-0.0024	0.0762	0.0031	-0.0004	0.0032	0.0014	0.0000	0.0031	0.0096	-0.0513
HAV	0.0004	0.0047	0.0031	0.0176	0.0130	0.0103	0.0000	0.0006	-0.0001	0.0034	-0.0082
KAV	-0.0060	0.0096	-0.0004	0.0130	0.0199	0.0127	-0.0011	0.0009	-0.0002	-0.0130	-0.0109
AAV	0.0034	0.0062	0.0032	0.0103	0.0127	0.0261	0.0003	0.0003	0.0001	-0.0062	-0.0031
HAA	0.0050	-0.0017	0.0014	0.0000	-0.0011	0.0003	0.0030	0.0003	0.0003	0.0039	-0.0023
KAA	0.0005	0.0042	0.0000	0.0006	0.0009	0.0003	0.0003	0.0009	0.0000	-0.0035	-0.0014
AAA	0.0002	-0.0012	0.0031	-0.0001	-0.0002	0.0001	0.0003	0.0000	0.0006	0.0014	-0.0039
PFK	0.0071	-0.0386	0.0096	0.0034	-0.0130	-0.0062	0.0039	-0.0035	0.0014	0.0593	-0.0108
PFA	-0.0017	0.0024	-0.0513	-0.0082	-0.0109	-0.0031	-0.0023	-0.0014	-0.0039	-0.0108	0.1559

Table 4
The matrix Σ_B^{-1}

	HAP	KAP	AAP	HAV	KAV	AAV	HAA	KAA	AAA	PFK	PFA
HAP	123.935	-98.957	-10.857	4.980	47.347	-27.258	-216.507	276.64	42.33	-40.832	-0.260
KAP	-98.957	247.853	2.286	-118.471	56.457	12.885	196.838	-610.68	89.30	143.125	3.529
AAP	-10.857	2.286	20.985	-4.841	3.728	-0.375	18.792	0.30	-79.23	1.990	5.217
HAV	4.980	-118.471	-4.841	271.428	-207.524	-13.379	23.830	28.72	-3.05	-140.770	-9.484
KAV	47.347	56.457	3.728	-207.524	274.286	-43.986	-78.865	47.47	64.91	107.257	16.598
AAV	-27.258	12.885	-0.375	-13.379	-43.986	67.356	16.997	8.96	-46.48	9.779	-3.215
HAA	-216.507	196.838	18.792	23.830	-78.865	16.997	839.194	-959.36	-145.11	25.869	-0.824
KAA	276.640	-610.684	0.298	28.715	47.474	8.965	-959.357	3693.55	-184.41	-132.624	22.104
AAA	42.329	89.297	-79.228	-3.054	64.909	-46.485	-145.110	-184.41	2537.67	22.786	36.932
PFK	-40.832	143.125	1.990	-140.770	107.257	9.779	25.869	-132.62	22.79	138.562	7.708
PFA	-0.260	3.529	5.217	-9.484	16.598	-3.215	-0.824	22.10	36.93	7.708	10.303

calculating $D^{(i)}$, this means $D^{(i)}$ tolerates more variation in PFA than in AAA. The largest negative covariance is that of normal ankle plantar/dorsiflexion pattern (AAP) and the primary frequency of the ankle plantar/dorsiflexion pattern (PFA) at -0.0513 . When interpreting covariances, it is standard practice to divide by the square root of the product of corresponding variances, thus obtaining correlation, a number forced to be between ± 1 . The correlation between AAP and PFA is equal to negative $0.0513 / (0.1559 \times 0.0762)^{1/2}$ or -0.47 . The negative correlation means that, when assessing an individual's gait pattern, if the solution of Eq. (3) gives a positive weight to AAP (the third component of $B^{(i)}$), then it is expected that the weighting of PFA (the last component of $B^{(i)}$), will be negative (or vice versa).

If the $B^{(i)}$ were to satisfy a multivariate normal distribution, then the values calculated for $D^{(i)}$ would be distributed as $F_{d, m-d+1} = F_{11, 338}$, where $d = 11$ is the dimension of the observations $B^{(i)}$, and $m = 348$ is the number of observations. The 90th, 95th and 99th percentiles of $F_{11, 338}$ are 1.62, 1.82 and 2.30 respectively, based on standard tables of the F distribution. Work reported in Wilson [16] investigated non-parametric bounds for the 95th percentile of $D^{(i)}$ values, which would be appropriate no matter what the underlying distribution of values $B^{(i)}$. Wilson chose 2.3 as the lower bound for 'abnormal' gait pattern: children with $D^{(i)}$ value greater than 2.3 display abnormal gait. Wilson chose 1.73 as the upper bound for 'normal' gait pattern; and values in the range $1.73 < D^{(i)} < 2.3$ were declared 'unusual' or suspicious, worth a second look. Note that these cut-off values are consistent with the theoretical F percentiles quoted above. Wilson's bounds have been chosen so as to minimize the probability of incorrectly classifying a child as either normal or abnormal, but at the cost of classifying some children as 'unusual'. There will always be a gray area requiring clinician input.

3. Results

To illustrate the application of the method, consider the two children identified as 8002 and 8570. The sagittal hip, knee and ankle data for these two cases are shown in Figs. 4–6, along with \pm two standard deviations

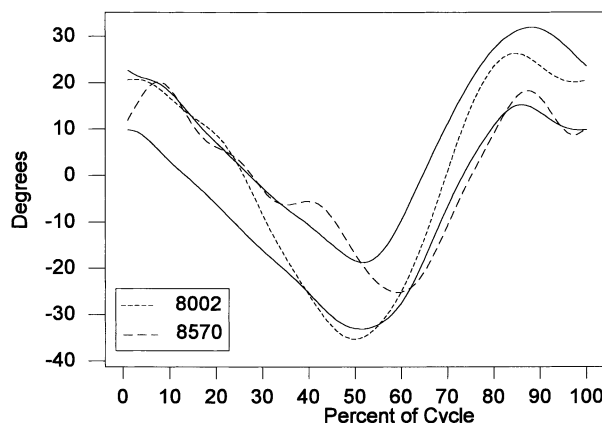


Fig. 4. Right hip angle patterns of children 8002 and 8570, and two standard deviation limits for mean pattern.

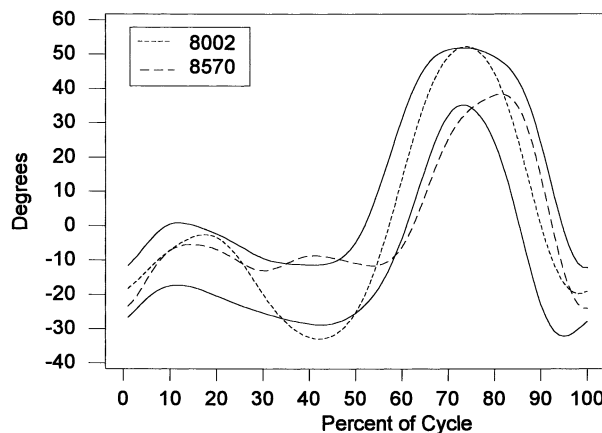


Fig. 5. Right knee angle patterns of children 8002 and 8570, and two standard deviation limits from mean pattern.

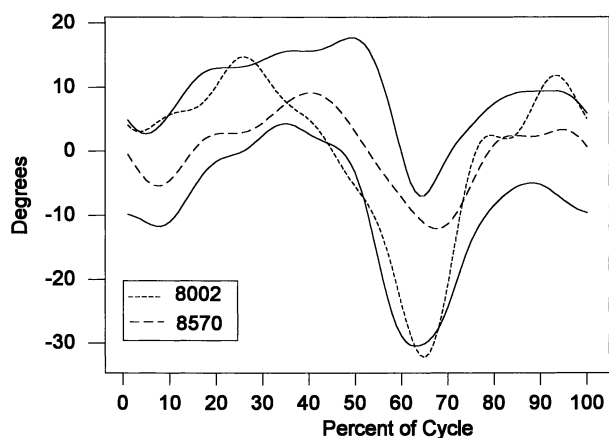


Fig. 6. Right ankle angle patterns of children 8002 and 8570, and two standard deviation limits for mean pattern.

tion limits from the mean curves. These limits were calculated at each percent of the cycle. The two standard deviation limits have been included to indicate population variability. Each child’s hip knee and ankle angle patterns were originally recorded as a total of roughly 60 data points (as in Fig. 1). The probability that all 60 of these points will lie within two standard deviations of the population mean curves is substantially lower than 95%, and most children’s angle patterns stray beyond the two standard deviation limits at some point.

Right side data for child 8002 are summarized in Table 5, to allow demonstration of the technique on known data. The 12 Fourier coefficients for hip, knee and ankle angle are displayed in the first three columns; the next column shows values of $B^{(8002)}$, and the fifth column shows standardized values of $B^{(8002)}$: values divided by the population standard deviation (square root of the corresponding entry on the diagonal of Table 3). The overall score for child 8002’s left side is $D^{(8002)} = 0.86$, well within normal bounds. But the right side measure is $D^{(8002)} = 1.85$, at the lower end of the

gray area between normal and abnormal. The largest standardized B values are 3.30, for knee angle pattern, and 2.3 for knee angle acceleration suggesting that, if there is a problem, then it lies in the child’s knee displacement curve. Fig. 5 shows the right knee displacement curve for Child 8002, overlaying the average \pm two standard deviations region. As can be seen, the child’s knee displacement curve falls outside the usual region in two places although not by very much, and the basic shape of the curve is surely normal. The ‘unusual’ gait score is detecting the fact that this child attains a larger range of knee flexion than most children.

The last column of Table 5 shows standardized B values for child 8570’s right side. This child’s overall score, on the right side, is $D^{(8570)} = 2.48$, well into the ‘abnormal’ range, and several standardized B values (HAP, KAP, HAV, HAA, KAA) are more than two standard deviations from mean behavior. This child’s hip pattern has an odd extra flexion bump in mid stance (Fig. 4), and the mid stance portion of the knee flexion curve remains flexed rather than extending to complete the knee flexion wave (Fig. 5). This child’s knee angle strays beyond the two standard deviation bounds but, unlike child 8002, the basic shape of 8570’s curve is abnormal. The score function D has been designed to detect such discrepancies in the shapes of curves. Note that the ankle pattern is roughly normal (Fig. 6), and indeed the standardized AAP value for $B^{(8570)}$ is 0.038, indicating that ankle pattern is very close to normal.

Other descriptors arising from this technique allow for more subtle analysis. The covariance matrix Σ_B indicates positive correlation between HAP and AAP, so one would expect the corresponding components of B to have the same sign. This is the case for child 8002, but not for child 8570. Similarly, Σ_B indicates that HAP and KAV usually have opposite signs, which is the case for child 8002, but not for child 8570. The score D defined by Eq. (4) in the Appendix A detects such

Table 5
Numeric data for children 8002 and 8570

	Hip 8002	Knee 8002	Ankle 8002	Right B 8002	Stand. right B 8002	Stand. right B 8570	
α_1	28.389	3.984	8.885	0.276	1.725	-2.610	HAP
α_2	-7.619	-21.895	-0.981	0.661	3.305	-2.844	KAP
α_3	-0.904	-1.423	-3.395	0.336	1.217	0.038	AAP
α_4	0.365	-0.590	2.925	-0.080	-0.600	-2.866	HAV
α_5	0.445	0.568	-0.227	-0.037	-0.262	-1.632	KAV
α_6	-0.146	0.283	-2.165	0.158	0.976	-0.289	AAV
β_1	-5.431	-28.535	10.746	0.002	0.031	-2.089	HAA
β_2	-1.861	9.786	-9.168	0.068	2.293	-2.493	KAA
β_3	1.384	3.578	-0.100	0.021	0.874	1.775	AAA
β_4	0.711	0.655	0.780	-0.482	-1.978	0.921	PFK
β_5	0.493	1.199	-2.287	0.062	0.157	-0.930	PFA
β_6	0.407	0.145	-0.261	-	-	-	

Table 6
Classification results for normal children less than 3 years of age

Age group	Number of records	Interpretable functions		PCs	
		Unusual (%)	Abnormal (%)	Unusual (%)	Abnormal (%)
1	98	15	75	6	74
1½	77	10	51	8	49
2	86	19	29	6	21
2½	70	19	16	4	16

abnormalities: child 8570 has unusual hip and knee angle patterns (standardized $B = -2.6$ and -2.8 , respectively); the ankle angle pattern is not unusual but, when considered in conjunction with the knee flexion, the gait measure flags child 8570 as abnormal.

It is this diagnostic capability of the interpretable functions which gives them an advantage over PCs in identifying the elements of the data which should be the focus of further investigation. The standardized vector B describes ‘standard deviations from the mean’ based on the overall pattern of the curves. As a result, values above 3.0 or below -3.0 certainly indicate unusual patterns. However, the measure $D^{(i)}$ can also detect a child for whom no individual standardized component is particularly unusual, but for whom the signs of those components are not consistent with the correlation patterns predicted by Σ_B .

The squared distance measure developed above for the 11 interpretable functions, was also applied to the eight PCs, with cutoffs for normal and abnormal derived using the same algorithms (Wilson [16]). Table 6 and Fig. 7 illustrate the technique applied to two groups of children who would be expected to have fairly large numbers classified as ‘abnormal’ when compared to the 3–7 year old group. Table 6 shows the results when applied to children under 3 years of age in the Sutherland [11] group of normal children. The results are as one would expect. Very young children, just learning to walk at age one, should look ‘abnormal’ relative to mature gait and indeed nearly 90% are classified as unusual or abnormal. The comparison with children at age 2.5 shows only 35% as unusual or abnormal. Applying the same procedure using PCs gives similar results.

Fig. 7 shows the results of the analysis applied to a group of children who were born prematurely (see Acknowledgements), using the same methodology as one would expect, more of these children are categorized as abnormal or unusual, with the proportion dropping off for older children. The two distance measures perform similarly, and show good discrimination. The 11 interpretable functions have the added advantage of diagnostic interpretation.

4. Discussion

We have presented a method for quantifying gait measurements which brings together two concepts. The first of these is the idea of having an overall ‘score’ for the gait patterns produced from an analysis which looks at the pattern of multiple curves simultaneously. The second concept is the use of ‘interpretable functions’ as an alternative to PCA. These interpretable functions explain about the same amount of the variation in the data as does PCA, but use as input the shapes of joint angle curves and the derivatives of those curves. In the presentation we have chosen to use the patterns of the sagittal plane joint angles since they are quite consistent across laboratories, regardless of the method of measurement. We also provide sufficient numerical data to be able to replicate our examples and to use new data to compute scores. For someone starting with a different set of ‘interpretable functions’, the procedure to determine scores would simply include the analysis of sufficient data to be able to estimate the appropriate covariance matrix. In fact, the weakest link of this type of gait analysis technique is that stable estimation of the covariance matrix requires data from many individuals.

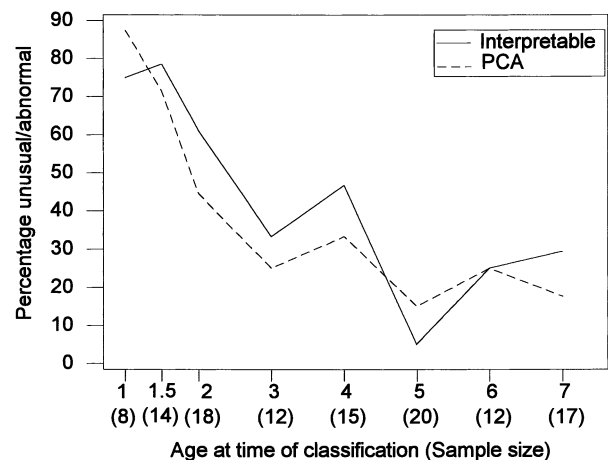


Fig. 7. Classification of children born prematurely, using two analyses with 11 interpretable functions and with 8 PCs.

The scores which we have computed should be considered in two parts. The $D^{(i)}$ score provides an overview of how the individual being tested fits into the distribution of people whose data made up the training sample. This number needs to be interpreted with care. Our analysis has been conservative in that many who would be identified as ‘unusual’ might be judged on a closer inspection to be within normal limits. On the other hand, the $D^{(i)}$ provides a quick method of screening. Once identified as ‘interesting’ by the $D^{(i)}$ calculation, an examination of standardized $B^{(i)}$ values tells which of the interpretable functions is producing the high value in $D^{(i)}$, or which values show unusual sign patterns. The power of the method is that it will identify equally well the person whose data is not terribly different from the mean in any one measurement but who has many measurements which are just a little odd (adding up to an overall pattern which doesn’t match the means), as well as a person who has a small number of very atypical results. Being able to examine $B^{(i)}$, and tell which functions lie close to and which lie far away from the mean, gives a direct link back to the original data for the person being tested, and points to which aspects of the gait cycle should be carefully observed by eye or on video. We believe this type of tool is valuable as a guide to which of the measured variables is likely to have the most clinical interest.

Acknowledgements

Data reported in this paper was collected by the Motion Analysis Laboratory, Children’s Hospital–San Diego under the Direction of Dr David H. Sutherland, MD. Funding for the original data collection was through NIH Grant 5 RO1 HD 08520 and for the study of children born prematurely was R01HD015801.

Appendix A

If a curve $f(t)$, $0 \leq t < 1$, is approximated by Fourier coefficients $\alpha_1, \dots, \alpha_6, \beta_1, \dots, \beta_6$, then

$$f(t) = \alpha_0 + \sum_{j=1}^6 [\alpha_j \cos(j2\pi t) + \beta_j \sin(j2\pi t)],$$

where $0 \leq t < 1$. (1)

(Some texts place a factor such as $1/(2\pi)$ in front of the summation sign, which amounts to rescaling all the Fourier coefficients.) If a curve $f(t)$ has been observed at T points t_1, \dots, t_T , with values $y_1 = f(t_1), \dots, y_T = f(t_T)$, then α_0 is the average of the y values, and

$$\gamma = (\alpha_1, \alpha_2, \dots, \alpha_6, \beta_1, \dots, \beta_6)$$

is the solution of the least squares regression problem with response vector the T observations

$$(y_1 - \alpha_0, y_2 - \alpha_0, \dots, y_T - \alpha_0)$$

and, for each $k = 1, \dots, T$, 12 predictor values:

$$(\cos(2\pi t_k), \cos(4\pi t_k), \dots, \cos(12\pi t_k), \sin(2\pi t_k), \sin(4\pi t_k), \dots, \sin(12\pi t_k)).$$

Then, each child’s three angle curves are summarized by a total of 36 Fourier coefficients:

$$\Gamma^{(i)} = (\gamma_h, \gamma_k, \gamma_a) \quad i = 1, \dots, 348,$$

where the subscripts denote hip, knee and ankle, respectively. The average of all 348 $\Gamma^{(i)}$ values is denoted $\bar{\Gamma}$ and the covariance matrix of these 348 vectors is a 36×36 matrix (not printed in this paper). The covariance matrix is calculated as:

$$(j,l) \text{ component of } \sum_{\Gamma} = \frac{1}{347} \sum_{i=1}^{348} (\Gamma^{(i)} - \bar{\Gamma})_j (\Gamma^{(i)} - \bar{\Gamma})_l,$$

$j, l = 1, 2, \dots, 36.$ (2)

The first diagonal entry of the covariance matrix stores the variance of the values of α_1 for the 348 observed hip curves. The last diagonal entry is the variance of the values of β_6 for the 348 observed ankle curves, etc. The off-diagonal entries store covariances between Fourier coefficients, across all three curves. The sum of the diagonal entries of the covariance matrix is the ‘total variation’ in the 348 vectors $\Gamma^{(i)}$ about their mean, $\bar{\Gamma}$. The first four (eight) PCs explain 72.7% (respectively, 85.7%) of the total variation. The eleven interpretable functions explain 74.8% of the total variation.

Table 1 lists the names of the 11 interpretable curves, and Table 2 gives the Fourier coefficients of these 11 curves. The 11 sets of 36 Fourier coefficients listed in Table 2 form a 36×11 matrix, Q . Each child’s vector $\Gamma^{(i)}$ (arranged as a column of 36 numbers) can be described in terms of its deviation about $\bar{\Gamma}$. This deviation is approximated as a linear combination of the 11 interpretable functions. The 11 coefficients of that linear combination are stored in $B^{(i)}$, which is the solution of yet another regression, and can describe as the least squares solution of the equation

$$\Gamma^{(i)} - \bar{\Gamma} = QB^{(i)}. \tag{3}$$

The covariances of the 348 observed $B^{(i)}$ are stored in the 11×11 matrix Σ_B , and printed in Table 3. The diagonal entries of Σ_B are the variances of the eleven components of the $B^{(i)}$, and the off-diagonal entries hold covariances. The inverse of matrix Σ_B is denoted Σ_B^{-1} , and is printed in Table 4. It is this last matrix that is needed to calculate the single number used to quantify a child’s gait as normal, unusual or abnormal. Note that the calculation of Σ_B^{-1} used a higher preci-

sion value of Σ_B than is printed in Table 3. The measure calculates a Hotelling's T-statistic (Seber [15]), rescaled to closely approximate an $F_{11, 338}$ distribution:

$$D^{(i)} = \frac{348 - 11 + 1}{348 \times 11} (\mathbf{B}^{(i)})^T \Sigma_B^{-1} \mathbf{B}^{(i)}. \quad (4)$$

References

- [1] Sutherland DH, Olshen RA, Biden EN, Wyatt MP. The development of mature walking. London: Mac Keith Press, 1988.
- [2] Winter DA. The biomechanics and motor control of human gait: normal, elderly and pathological. University of Waterloo Press, 1991.
- [3] Lasko P, Beuter A, Biden E. Kinematic variability and relationships characterizing the development of coordinative structure for human walking. *Dev Psychobiol* 1990;23(8):809–37.
- [4] Deluzio KD, Wyss UP, Zee B, Costigan PA, Sorbie C. Principal component models of knee kinematics and kinetics: normal vs. pathological gait patterns. *Hum Movement Sci* 1997;16:201–17.
- [5] Sadeghi H, Prince F, Sadeghi S, LaBelle H. Principal component analysis of the power developed in the flexion/extension muscles of the hip in able-bodied gait. *Med Eng Phy* 2000;22:703–10.
- [6] Olney S, Griffin M, McBride I. Multivariate examination of data from gait analysis of persons with stroke. *Physical Therapy* 1998;78(8):814–28.
- [7] Schutte L, Narayanan U, Stout J, Sleber P, Gage J, Schwartz M. An index for quantifying deviations from normal gait. *Gait and Posture* 2000;11:25–31.
- [8] Schwartz M, Novacheck T, Trost J. A tool for quantifying hip flexor function during gait. *Gait and Posture* 2000;12:122–7.
- [9] Biden E, Olshen R, Simon S, Sutherland D, Gage J, Kadaba M. Comparison of gait data from multiple labs. *Trans Orthopaedic Res Soc* 1987;Jan.
- [10] Granata K, Abel M, Damiano D. Joint angular velocity in spastic gait and the influence of muscle-tendon lengthening. *J Bone Joint Sur* 2000;82:174–86.
- [11] Sutherland DH, Olshen R, Cooper L, Woo SL-Y. The development of mature gait. *J Bone Joint Sur* 1980;62A:336–53.
- [12] Capozzo A, Leo T, Pedotti A. A general computing method for the analysis of human locomotion. *J Biomech* 1975;8:307–20.
- [13] Olshen RA, Biden EN, Wyatt MP, Sutherland DH. Gait analysis and the bootstrap. *Ann Stat* 1989;17(4):1419–40.
- [14] Biden E, O'Connor J, Collins JJ. Gait analysis. In: Daniel D, Akeson W, O'Connor J, editors. *Knee ligaments, structure function injury and repair*. Raven Press, 1990:291–311.
- [15] Seber GAF. *Multivariate observations*. New York: Wiley, 1984.
- [16] Wilson CD. An analysis of the patterns of variation in the gait of normal children, aged three to seven, MSc Thesis, University of New Brunswick, Fredericton; 1998.